Detecting zero-line mode in bilayer graphene via the quantum Hall effect

Ying-Tao Zhang,[1] Zhenhua Qiao,[2,3] and Qing-Feng Sun[4,5]

[1]*College of Physics, Hebei Normal University, Shijiazhuang 050016, China*

[2]*Department of Physics, The University of Texas at Austin, Austin, Texas 78712, USA*

[3]*ICQD, Hefei National Laboratory for Physical Sciences at Microscale, University of Science and Technology of China,
Hefei, Anhui 230026, China*

[4]*Institute of Physics, Chinese Academy of Sciences, Beijing 100190, China*

[5]*International Center for Quantum Materials, School of Physics, Peking University, Beijing 100871, China*

The zero-line mode can be produced in AB-stacking bilayer graphene under a spatially varying electric field. We investigate the transport properties of the zero-line mode in a six-terminal Hall bar system in the presence of a uniform magnetic field. We find that the Hall resistance is zero and the longitudinal resistance exhibits a plateau with $1/2(h/2e^2)$, when the Fermi level lies between the lowest conduction and highest valence Landau levels, which corresponds to the zero-line modes. Since the zero-line mode propagates along the domain wall separating opposite valley-Hall topologies, we also numerically measure the currents between source and drain and the conductance between two of the transversal terminals. Our finding shows that the current between source and drain is due to the existence of kink state, which can serve as a scheme to detect the zero-line mode. We further show that the zero-line mode under strong magnetic field is robust against disorders.

PACS number(s): 71.20.−b, 73.23.Ad, 73.43.−f, 72.80.Vp

I. INTRODUCTION

After the discovery of graphene,[1–3] the study of graphene-based systems becomes one of the most interesting and active topics in material physics.[4–6] Since an externally tunable band gap can be easily engineered in AB stacked bilayer graphene through applying a vertical electric field,[7,8] bilayer graphene provides a better platform to fabricate graphene-based electronics.[9,10] Whenever the applied electric field changes its sign spatially in bilayer graphene, a chirally propagating zero-line mode can be produced to localize along the paths determined by opposite valley-Hall topologies,[11,12] which corresponds to "kink states" in the band spectrum. Based on the creation of a zero-line mode by an asymmetric potential profile, Martin *et al.*[11] have discussed its relevance to valleytronics[13] by utilizing the valley degrees of freedom. The zero-line mode is also found to exhibit a zero bend resistance and is robust against weak disorders due to the wide spread of wave functions.[12,14] Such a one-dimensional conducting mode has also been reported in other systems.[15–25] Killi *et al.*[15] demonstrated that the periodic supercell can result in zero-energy anisotropic massless Dirac fermions and finite energy Dirac points with tunable velocities. Moreover, how the zero-line mode is influenced by a magnetic field has been studied, and the results can serve as a possible route to fabricate a switchable one-way valley filter.[16] The tunable Luttinger liquid[26] has been proposed in the localized chiral zero-line state. The zero-line mode at topological intersections is shown to obey a counterintuitive current partition law.[27] However, so far, no experimental report has demonstrated the existence of the zero-line mode in bilayer graphene.

In this work, we investigate the transport properties of a six-terminal bilayer graphene Hall bar system, where a vertical electric field is applied and the electric field is assumed to have the same strength but opposite signs in the upper and lower parts of the device [see Fig. 1]. The zero-line mode arises under such an electric field distribution.[11] In our studied system, the horizontal direction (including 1 and 4 terminals) displays zigzag-terminated boundaries, while the transversal terminals 2, 3, 5, and 6 have armchair-terminated boundaries. Here, we want to point out that the zero-line mode is different with the zero-energy states localized at the edges in zigzag graphene ribbons and triangular dots, the latter originates from the breaking of the sublattice symmetry between the two types of atoms in the unit cell of the graphene honeycomb lattice. The zero-line mode is independent of zigzag interfaces, which can be produced in any kind of interfaces of bilayer graphene ribbons.[12,14] By further considering a strong magnetic field, we show that the existence of the zero-line mode can be readily observed through measuring the Hall and longitudinal resistances.

II. MODEL AND METHOD

In the tight-binding representation, the π-orbital Hamiltonian of a gated bilayer graphene in the presence of strong magnetic field can be written as

$$
\begin{aligned}
H = & \sum_{i \in T} (+U + \varepsilon_i) c_i^\dagger c_i + \sum_{i \in B} (-U + \varepsilon_i) c_i^\dagger c_i \\
& + \sum_{\langle i,j \in T(B) \rangle} t e^{i\phi_{ij}} c_i^\dagger c_j \\
& + t_\perp \sum_{\langle i \in T, j \in B \rangle} (c_i^\dagger c_j + \text{H.c.}),
\end{aligned} \tag{1}
$$

where $t = 2.8$ eV is the nearest-neighbor hopping energy—it is chosen as the unit of energy in the following. $c_i^\dagger$ (c_i) creates (annihilates) an electron on site i, $2U$ represents the interlayer potential difference. ε_i is the on-site disorder potential, which is uniformly distributed in the range of $[-W/2, W/2]$ with disorder strength W. Under the influence of a perpendicular magnetic field B, the nearest-neighbor hopping term is replaced by a Peierls substitution $t \rightarrow t e^{i\phi_{ij}}$, where
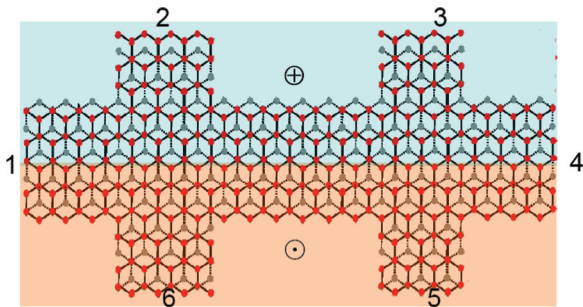
FIG. 1. (Color online) Schematic plot of a six-terminal bilayer graphene Hall bar. Opposite perpendicular electric fields are applied in the upper and lower regions, where $\oplus$ and $\odot$ denote vertically downward and upward electric fields, respectively.

$\phi_{ij} = \int_i^j \vec{A} \cdot d\vec{l}/\phi_0$ with $\phi_0 = \hbar/e$ is the quantum of flux. Here, we choose the vector potential in the form of $\vec{A} = (-By,0,0)$. $t_\perp$ couples directly between the A sites at the top layer and the B sites at the bottom layer. Note that other interlayer hopping terms are neglected since they have no significant effects on the Landau levels of bilayer graphene.[28–30] We set the distance between two nearest-neighbor sites as the unit of length in our calculations.

The current I_p of lead p is determined by the multiterminal Landauer-Büttiker formula and is given as

$$I_p = \frac{e}{h} \sum_{q(q \neq p)} T_{pq}(V_p - V_q), \qquad (2)$$

where V_i is the potential at lead i, and T_{pq} is the transmission coefficient for electrons from lead q to lead p, which can be calculated from[31]

$$T_{pq} = \text{Tr}[\Gamma_p G^r \Gamma_q G^a], \qquad (3)$$

where $\Gamma_p = i[\Sigma_p^r - \Sigma_p^a]$ is the linewidth function coupling the semi-infinite lead with the central scattering regime. $G^r = [E - H_C - \Sigma_p^r]^{-1}$ is the retarded Green function, where H_C is the Hamiltonian in the central region. $\Sigma_p^{r,a}$ is the self-energy of lead p, which can be calculated numerically.[32] The width of the sample is denoted by N (e.g., in Fig. 1, the system size is $N = 2$).

III. NUMERICAL RESULTS

In our following simulations, we choose the system to be $N = 75$, which corresponds to a width of 320-Å bilayer graphene ribbon. The magnetic flux ϕ in the honeycomb lattice is fixed at 0.007 and the interlayer hopping energy $t_\perp$ is set to be $0.3t$.[28,33] Figure 2 displays the band structure of the system. Under an interlayer potential difference U, the zero-energy Landau level exhibits a large splitting around U in which the layer (valley) degeneracy is lifted.[8,28,29] However, at the energy spectrum shown in Fig. 2, there are eight edge states (e.g., states labeled as "A"–"H") when the Fermi level is located between the lowest conduction and highest valence Landau levels. The corresponding wave-function distributions across the transverse direction are plotted in Fig. 3. One can observe that the states of "A" and "H" ("D" and "E") are oppositely localized at the boundaries, and it is known that these states are boundary dependent and can only propagate
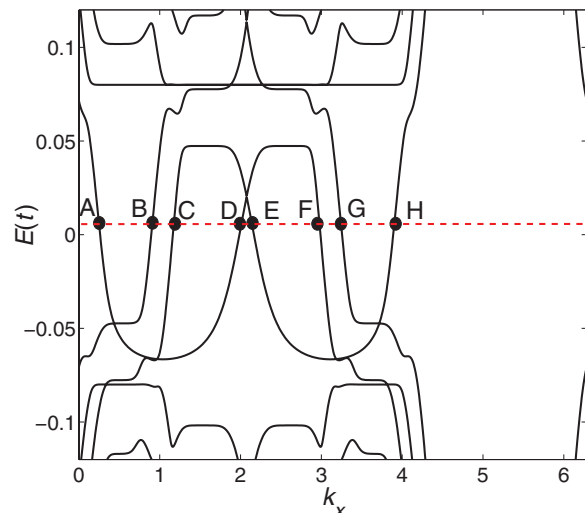

FIG. 2. (Color online) Band structure of the zero-line mode in the presence of a strong magnetic field. Here, the interlayer potential difference is chosen to be $U = 0.08t$. The sample width is set as $N = 75$ and the magnetic flux is $\phi = 0.007$.

along ribbons where valleys are separated and intervalley scattering is weak.[12] From Fig. 3, one can find that there also exist four states (B, G, C, and F) also named as zero-line states localized at the center of the system or the line where the interlayer potential difference changes its sign. Here, we only present the band structure and wave-function distribution of edge modes of the zigzag-terminated bilayer graphene nanoribbon. Actually, the zero-line states in the presence of magnetic field also arise in the armchair-terminated bilayer graphene nanoribbon, which are independent of the edge configurations.

Based on the energy dispersion and the wave-function distribution, one can reach a clear picture of the zero-line mode
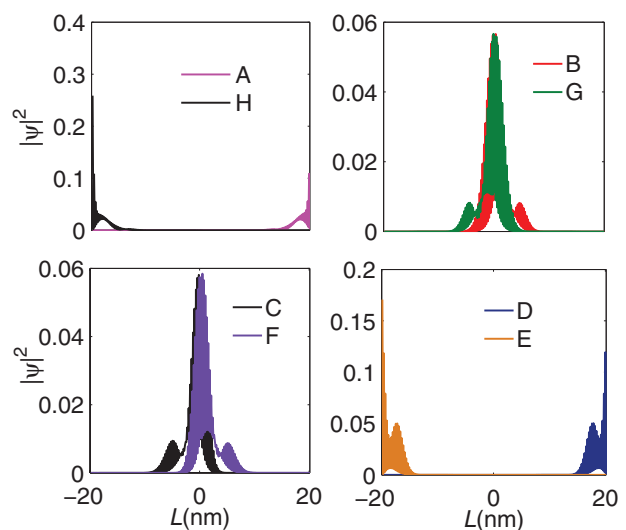

FIG. 3. (Color online) Wave function distribution of the states "A"–"H" labeled in Fig. 2. States A, H, D, and E correspond to the edge modes that can only propagate along boundaries without intervalley scattering. B, G, C, and F are for the zero-line modes that emerged from the sign change of the applied electric field.
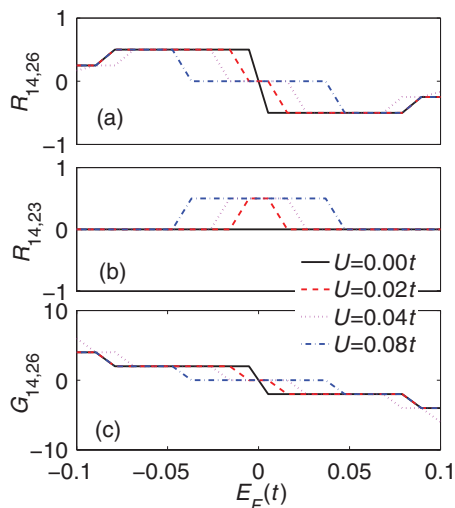
FIG. 4. (Color online) Hall resistance $R_{14,26}$, the longitudinal resistance $R_{14,23}$, and the longitudinal conductance as a function of the Fermi energy E_F. Here, the parameters are $N = 75$ and $\phi = 0.007$. The unit of the Hall and longitudinal resistances is $h/2e^2$.

FIG. 5. (Color online) The resistance $R_{14,14}$ and the conductances $G_{23,23}$ and $G_{32,32}$ as a function of Fermi energy E_F. The parameters of $N = 70$ and $\phi = 0.007$ are used. The unit of the resistance is $h/2e^2$ and the unit of the conductance is $2e^2/h$.

in the considered system. When the Fermi energy lies inside the lowest conduction and highest valence Landau levels, one pair of the zero-line states transverses along the central region from left to right. This is intuitively illustrated in Fig. 1. Therefore the current between terminals 1 and 4 is nonzero. Moreover, the existence of the zero-line mode can affect the transport properties of the longitudinal and Hall resistances.

When a small external bias is applied between lead 1 and lead 4, by requiring the zero charge currents of transverse terminals 2, 3, 5, and 6 (working as voltage probes), the voltage V_p ($p = 2,3,5,6$) can be obtained. Then the longitudinal resistance $R_{14,23} = (V_2 - V_3)/I_{14}$ and the Hall resistance $R_{14,26} = (V_2 - V_6)/I_{14}$ can be calculated. In our calculations, we set the width of transversal terminals to be 123 Å, which is much larger than the magnetic length. In Fig. 4, we plot the longitudinal and Hall resistances of the considered system as a function of the Fermi energy for different interlayer potential differences, i.e., $U/t = 0.00,0.02,0.04,0.08$. One can see that the Hall resistance $R_{14,26}$ is zero when the Fermi energy is between the lowest electron and hole Landau levels, and for the Fermi energies beyond, the Hall resistance exhibits quantized plateaus with values $\pm 1/2(h/2e^2)$, $\pm 1/3(h/2e^2)$, etc. The nonzero Hall resistance can be represented by $R_{14,26} = 1/\nu(h/2e^2)$, where ν is the filling factor. In this case, ν is zero and the Hall resistance $R_{14,26}$ shows a zero plateau, which is completely distinct from those in bilayer graphene with uniformly distributed interlayer potential difference.[28] In addition, one can see that the longitudinal resistance shows a plateau with $1/2(h/2e^2)$ while the Fermi energy is between the lowest electron and hole Landau levels. From the analysis of edge states in Figs. 2 and 3, we know that states labeled A, H, D, and E can only propagate along sample boundaries, which give zero contribution to the longitudinal resistance.[28] Only the zero-line modes B, G, C, and F contribute to the quantized longitudinal resistance. Because the number of counterpropagating zero-line mode pairs is 2, the longitudinal resistance plateau shows the value of $1/2(h/2e^2)$. The quantization and
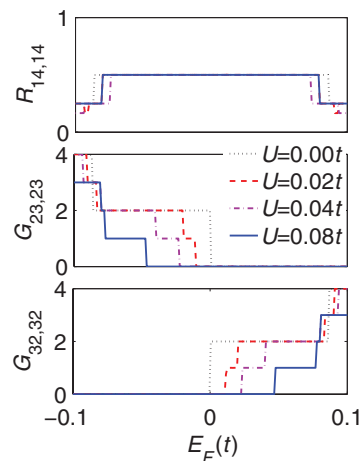
robustness of the zero-line mode arise from the chirality of the zero-line mode. For Fermi energies beyond, the longitudinal resistance shows a zero plateau. Therefore such zero Hall and half-quantized longitudinal resistances should arise from the contribution of the zero-line mode.

In the above discussions, we have studied the effect of the zero-line mode on the longitudinal and Hall resistances. However, it is still yet enough to probe the existence of the zero-line state in the considered system. We know that the zero-line mode propagates along the middle interface, therefore we measure the current between terminals 1 and 4 to probe it. In Fig. 5, one can see that the resistance $R_{14,14}$ shows plateaus of $\pm 1/2(h/2e^2)$, $\pm 1/3(h/2e^2)$, etc., which prove the existence of current between terminals 1 and 4. One may wonder whether the current propagates along the sample boundaries. In Fig. 5, we also present the conductance $G_{23,23} = I_{23}/V_{23}$ between terminals 2 and 3, where the voltage of terminal 2 is set to be V and that of other terminals is set to be 0. Similarly, the conductance $G_{32,32} = I_{32}/V_{32}$ is also presented. One can observe that both $G_{23,23}$ and $G_{32,32}$ give zero value plateau when the Fermi energy is between the lowest electron and hole Landau levels. This indicates that the current does not propagate along the sample boundaries. Therefore the current between terminals 1 and 4 comes from the contribution of the zero-line mode. When the Fermi energy is beyond the lowest electron and hole Landau levels, $G_{23,23}$ and $G_{32,32}$ show integral quantum conductance plateau values with $1(2e^2/h)$, $2(2e^2/h)$, $3(2e^2/h)$, etc.

Till now, we have presented a scheme of probing the existence of a kink state by ways of measuring the longitudinal and Hall resistances. One may also wonder whether the zero-line mode discussed above is robust against disorders or whether the considered scheme is feasible in experiment. To this end, in Fig. 6, we explore the disorder effect on the longitudinal resistance $R_{14,14}$. In the numerical calculation, up to 200 ensembles are collected to for each point. In the absence of disorder (i.e., $W = 0$), $R_{14,14}$ shows quantum conductance plateaus in units of $1/2(h/2e^2)$ and $1/3(h/2e^2)$. When the disorder is present, one can notice that only small fluctuations
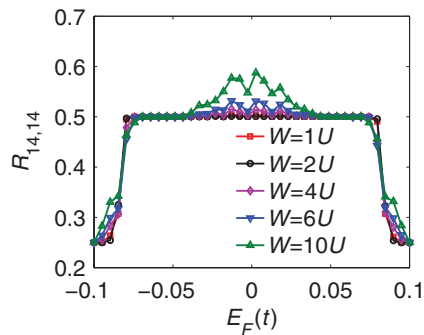
FIG. 6. (Color online) The resistance $R_{14,14}$ as a function of the Fermi energy E_F for different disorder strengths W. Other parameters used are the same as those in Fig. 5.

are imposed on the plateau $1/2(h/2e^2)$ for $W = 1U$, $2U$, and $4U$. Such observations demonstrate that the zero-line mode is much robust against disorder, which is due to their spatial wave-function distribution.[12] Furthermore, one can see that the resistance $R_{14,14}$ contributed by the zero-line states becomes large when the disorder strength reaches $W = 6U$ or $10U$, and the quantum plateau with value $1/2(h/2e^2)$ is destroyed. The reason behind is that the zero-line mode is located in the central region of the sample, and it is produced within a bulk gap. Since an extremely large disorder destroys the bulk gap, the zero-line mode is also destroyed along with the breaking of the bulk band gap.

Here, we would like to point out that counterpropagating zero-line modes are encoded with different valleys K and K' in the absence of an external magnetic field. Whenever the disorder is smooth, no backscattering is allowed. Therefore only the short-range disorder can possibly scatter the zero-line mode. In the presence of magnetic field, it can form Landau levels. However, the zero-line mode here still comes

from the opposite electric field, which is not affected by the presence of a magnetic field. Therefore this zero-line mode should still be robust against smooth (or long-range) disorders.

IV. CONCLUSIONS

In summary, in a six-terminal Hall bar setup, we have investigated the effect of the zero-line mode on the quantum Hall effect in a bilayer graphene experiencing a spatially varying interlayer potential difference. Due to the existence of the zero-line mode in bilayer graphene, the Hall resistance shows zero value plateaus and the longitudinal resistance shows a plateau with $1/2(h/2e^2)$ when the Fermi energy lies between the lowest conduction and highest valence Landau levels. Moreover, our numerical results demonstrate that the current between horizontal terminals flows along the middle interface, which is the characteristic of the zero-line mode in gated bilayer graphene. Thus our proposed scheme can be used to probe the existence of the zero-line mode due to the presence of opposite valley-Hall topologies. Furthermore, we numerically show that the zero-line mode is very robust against the short-range Anderson disorder, which is thus feasible in experiment.

[1] K. S. Novoselov, A. K. Geim, S. V. Morozov, D. Jiang, M. I. Katsnelson, I. V. Grigorieva, S. V. Dubonos, and A. A. Firsov, Nature (London) **438**, 197 (2005).

[2] Y. B. Zhang, Y.-W. Tan, H. L. Stormer, and P. Kim, Nature (London) **438**, 201 (2005).

[3] K. S. Novoselov, E. McCann, S. V. Morozov, V. I. Falko, M. I. Katsnelson, U. Zeitler, D. Jiang, F. Schedin, and A. K. Geim, Nat. Phys. **2**, 177 (2006).

[4] A. H. Castro-Neto, F. Guinea, N. M. R. Peres, K. S. Novoselov, and A. K. Geim, Rev. Mod. Phys. **81**, 109 (2009), and references therein.

[5] N. M. R. Peres, Rev. Mod. Phys. **82**, 2673 (2010).

[6] S. Das Sarma, S. Adam, E. H. Hwang, and E. Rossi, Rev. Mod. Phys. **83**, 407 (2011).

[7] Y. B. Zhang, T. T. Tang, C. Girit, Z. Hao, M. C. Martin, A. Zettl, M. F. Crommie, Y. R. Shen, and F. Wang, Nature (London) **459**, 820 (2009).

[8] E. V. Castro, K. S. Novoselov, S. V. Morozov, N. M. R. Peres, J. M. B. Lopes dos Santos, Johan Nilsson, F. Guinea, A. K. Geim, and A. H. Castro Neto, Phys. Rev. Lett. **99**, 216802 (2007).

[9] A. S. Mayorov, D. C. Elias, M. Mucha-Kruczynski, R. V. Gorbachev, T. Tudorovskiy, A. Zhukov, S. V. Morozov, M. I.

Katsnelson, V. I. Falko, A. K. Geim, and K. S. Novoselov, Science **333**, 860 (2011).

[10] E. McCann and M. Koshino, Rep. Prog. Phys. **76**, 056503 (2013).

[11] I. Martin, Ya. M. Blanter, and A. F. Morpurgo, Phys. Rev. Lett. **100**, 036804 (2008).

[12] Z. Qiao, J. Jung, Q. Niu, and A. H. MacDonald, Nano Lett. **11**, 3453 (2011).

[13] A. Rycerz, J. Tworzydlo, and W. C. Beenakker, Nat. Phys. **3**, 172 (2007).

[14] J. Jung, Z. H. Qiao, Q. Niu, and A. H. MacDonald, Nano Lett. **12**, 2936 (2012).

[15] M. Killi, S. Wu, and A. Paramekanti, Phys. Rev. Lett. **107**, 086801 (2011).

[16] S. Wu, M. Killi, and A. Paramekanti, Phys. Rev. B **85**, 195404 (2012).

[17] R. Jackiw and C. Rebbi, Phys. Rev. D **13**, 3398 (1976).

[18] W. P. Su, J. R. Schrieffer, and A. J. Heeger, Phys. Rev. Lett. **42**, 1698 (1979).

[19] G. W. Semenoff, V. Semenoff, and F. Zhou, Phys. Rev. Lett. **101**, 087204 (2008).

[20] W. Yao, S. A. Yang, and Q. Niu, Phys. Rev. Lett. **102**, 096801 (2009).

[21] Y. Ran, Y. Zhang, and A. Vishwanath, Nat. Phys. **5**, 298 (2009).

[22] G. E. Volovik, *The Universe in a Helium Droplet* (Oxfdord University Press, Oxford, UK, 2003).

[23] T. Ochiai and M. Onoda, Phys. Rev. B **80**, 155103 (2009).

[24] A. B. Khanikaev, S. H. Mousavi, W.-K. Tse, M. Kargarian, A. H. MacDonald, and G. Shvets, Nat. Mater. **12**, 233 (2013).

[25] J. Song, H. Liu, H. Jiang, Q.-F. Sun, and X. C. Xie, Phys. Rev. B **86**, 085437 (2012).

[26] M. Killi, T. C. Wei, I. Affleck, and A. Paramekanti, Phys. Rev. Lett. **104**, 216406 (2010).

[27] Z. H. Qiao, J. Jung, C. W. Lin, A. H. MacDonald, and Q. Niu, arXiv:1302.6307.

[28] Y. T. Zhang, X. C. Xie, and Q. F. Sun, Phys. Rev. B **86**, 035447 (2012).

[29] E. McCann and V. I. Falko, Phys. Rev. Lett. **96**, 086805 (2006).

[30] F. Guinea, A. H. Castro Neto, and N. M. R. Peres, Phys. Rev. B **73**, 245426 (2006)

[31] *Electronic Transport in Mesoscopic Systems*, edited by S. Datta (Cambridge University Press, Cambridge, UK, 1995).

[32] D. H. Lee and J. D. Joannopoulos, Phys. Rev. B **23**, 4997 (1981).

[33] W. Long, Q.-F. Sun, and J. Wang, Phys. Rev. Lett. **101**, 166806 (2008).